

RSC Advances



This is an *Accepted Manuscript*, which has been through the Royal Society of Chemistry peer review process and has been accepted for publication.

Accepted Manuscripts are published online shortly after acceptance, before technical editing, formatting and proof reading. Using this free service, authors can make their results available to the community, in citable form, before we publish the edited article. This *Accepted Manuscript* will be replaced by the edited, formatted and paginated article as soon as this is available.

You can find more information about *Accepted Manuscripts* in the [Information for Authors](#).

Please note that technical editing may introduce minor changes to the text and/or graphics, which may alter content. The journal's standard [Terms & Conditions](#) and the [Ethical guidelines](#) still apply. In no event shall the Royal Society of Chemistry be held responsible for any errors or omissions in this *Accepted Manuscript* or any consequences arising from the use of any information it contains.

ARTICLE

Theoretical investigation on Atomic Oxygen Erosion Mechanisms of 1, 3 - Didecyl Cyclopentane, 1, 3 - Dioctyldodecyl Cyclopentane and Alkylated Cyclopentane

Cite this: DOI: 10.1039/x0xx00000x

Received 00th January 2012,
Accepted 00th January 2012

DOI: 10.1039/x0xx00000x

www.rsc.org/

Jingyan Nian,^a Ping Gao,^a Yongcheng Wang,^c Zhiguang Guo,^{a,b,*} Weimin Liu^a

The micro erosion processes of atomic oxygen for 1, 3 - didecyl cyclopentane and 1, 3 - dioctyldodecyl cyclopentane lubricants have been investigated by using Reaxff molecular dynamics method. Simulation results showed that the creating of H₂, CO, CO₂ is the main reason for the quality loss of lubricants. O-atom addition and H abstraction are the main mechanisms. Furthermore, singlet and triplet atomic oxygen erosion mechanisms for two kinds of alkylated cyclopentanes have been investigated utilizing density functional theory (DFT) methods. DFT calculation demonstrated that different spin states atomic oxygen correspond to different erosion mechanisms, and no non-adiabatic reaction phenomenon appears. Alkylated cyclopentanes are damaged by inserting of triplet oxygen atoms among the C-C bonds, the branched chain in alkylated cyclopentane is easier to be taken off due to the lower activation barrier. Erosion products are H, CO, CO₂, CH₂O, organic oxygen radicals are the main intermediates in ³O erosion process. However, ¹O erosion originates from the elimination mechanism and the extent of lubricant degradation is slighter. Finally, the diffusion coefficient of atomic oxygen in 1, 3 - didecyl cyclopentane is 1.63 time than 1, 3 - dioctyldodecyl cyclopentane as the fundamental reason for the 1, 3-dioctyldodecyl cyclopentane with the better atomic oxygen resistance performance was discovered.

ARTICLE

Introduction

The international space station (ISS), the space shuttle, and many other satellites circumnavigate Earth at altitudes of 180-650 km above its surface, in low Earth orbit (LEO). The largest component of the low Earth orbit is atomic oxygen (AO).¹ This highly reactive species is formed when oxygen and ozone molecules are split by solar ultraviolet radiation in an environment where the mean free path is sufficiently large caused by ultra-high vacuum that the probability of recombination is negligible. Oxygen atoms hit a spacecraft surface with mean impact energies of approximately 4.5 eV (103.8 kcal/mol) with the energy spread of about 50 kcal/mol.² Materials of spacecraft are damaged seriously because of the high collision energy and temperature.³⁻⁹ Space lubricant as one fragment of spacecraft and its function is vital and it subjects to atomic oxygen erosion will cause the lubrication failure and lead to great loss. With the in-depth research to space liquid lubricants, the atomic oxygen erosion mechanism has attracted people's attention.¹⁰⁻¹⁶

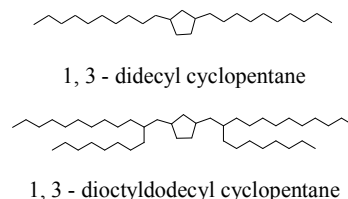
Multiply alkylated cyclopentane lubricants¹⁷ are synthesized by reacting cyclopentadiene with various alcohols in the presence of a strong base. The reaction products are then hydrogenated to produce the final product, which is a mixture of di-, tri-, tetra-, or penta-alkylated cyclopentanes. Our laboratory has synthesized 1, 3 - didecyl cyclopentane and 1, 3 - dioctyldecyl cyclopentane lubricants^{18,19} and investigated their lubrication performance, the results demonstrated that they are hopeful to replace the perfluoropolyether (PFPE) as a new generation of space liquid lubricant due to its high bearing capacity, lower temperature viscosity, the lower saturated vapour pressure (9.1×10^{-7} Pa and 7.5×10^{-7} Pa respectively at 298 K compared with the space lubricant NYE (USA) of 1.3×10^{-5} Pa), no corrosion for friction pair. This conclusion has also been verified by us using computational chemistry method and the details shown in **Electronic Supplementary Information** of this paper. Furthermore, under the atomic oxygen surrounding, two kinds of lubricants have also been investigated by using home-made multifunctional space tribology experimental system. The experimental results indicated that the quality loss of lubricants leads to lubrication degradation. Moreover, 1, 3 - dioctyldecyl cyclopentane has the better performance in preventing of atomic oxygen erosion.¹⁹ However, the essences of quality loss and 1, 3 - dioctyldecyl cyclopentane has the better performance in preventing of atomic oxygen have still been unclear and puzzled us in the experimental conditions. Meanwhile, previous studies mainly focused on the atomic oxygen erosion mechanism of simple organic molecules such as methane^{20,21} and ethane.^{22,23} Herein, atomic oxygen erosion mechanisms investigation for alkylated cyclic hydrocarbon will be meaningful.

It is worth mentioning that large numbers of researches showed that non-adiabatic reaction process caused by spin-orbit coupling occurs in multi-spin states transition metal systems.²⁴⁻²⁹ The existence of ¹O and ³O in low earth orbital has a great possibility due to the extra energy supplied by ultraviolet. The appearance of non-adiabatic reaction process or not during the course of atomic oxygen erosion also aroused our interest.

Therefore, in this work, the atomic oxygen erosion mechanisms of two kinds of space lubricants will be investigated through Reaxff molecular dynamics calculation, and ¹⁸O erosion mechanism of two kinds of alkylated cyclopentane will be studied by using the DFT method. The essence of 1, 3 -dioctyldecyl cyclopentane has the better performance in preventing of atomic oxygen erosion will as focus to be investigated. Moreover, non-adiabatic phenomenon in atomic erosion process will be discussed.

Methods and Computational details

1, 3 - didecyl cyclopentane and 1, 3 - dioctyldecyl cyclopentane space lubricants as research objects are shown as follows:



ReaxFF³⁰ is a potential based on quantum mechanics that can simulate chemical reactions of materials. It uses a general relationship between bond distance and bond order, which determines bond energy, and can give a proper description of the dissociation and formation of bonds between atoms.³¹⁻³⁵ We employ the reactive force field (ReaxFF 6.0), which is included in GULP package in the version of Material studio 6.0 and use parameters to simulate the large amounts of atomic oxygen erosion process for 1, 3 - didecyl cyclopentane and 1, 3 - dioctyldecyl cyclopentane.

The layer structure (see the initial layer structure in Fig 2) belongs to space group of Triclinic P_1 in which one 1, 3 - didecyl cyclopentane or 1, 3 - dioctyldecyl cyclopentane with two hundred atomic oxygen are embraced. Lattice parameters $a = 15 \text{ \AA}$, $b = 30 \text{ \AA}$, $\alpha = \beta = \gamma = 90^\circ$ and 20 \AA vacuum layer was added to the upper of the cell. The densities of 1, 3 - didecyl cyclopentane and 1, 3 - dioctyldecyl cyclopentane are 0.85 g/cc and 0.9 g/cc respectively. The geometries optimizations were carried out utilizing Forcite and GULP modules with the COMPASS³⁶ and ReaxFF 6.0 force field respectively. All MD simulation was carried out with the NVE ensemble at the 298 K, and equilibration time and total simulation time were 1ps and 10 ps, and time step was set as 0.5 fs.

To calculate the diffusion coefficient, two amorphous cells were constructed respectively embracing ten 1, 3 - didecyl cyclopentane or 1, 3 - dioctyldecyl cyclopentane with four atomic oxygen. We performed a short energy minimization to optimize the cell. After the minimization, five annealing cycles calculation on the optimized structure was carried out, the initial temperature is 300 K, and the mid-cycle temperature is 500 K. The annealed results are shown as Fig 1(a, b).

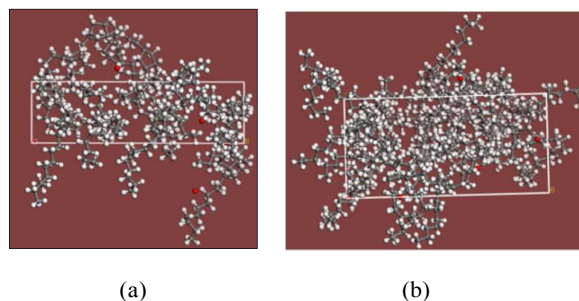


Fig1. (a): Annealed amorphous cell embraces ten 1, 3 - didecyl cyclopentane with four atomic oxygen. (b): Annealed amorphous cell embraces ten 1, 3 - dioctyldecyl cyclopentane with four atomic oxygen.

Finally, the 30 ps MD simulation was performed under the NVE ensemble with the COMPASS force field³⁶ at 298 K.

The mean square displacement is defined as formula 1:

$$MSD = \langle [r_i(t) - r_i(0)]^2 \rangle \quad (1)$$

$r_i(t)$ is the displacement vector at t time, and $\langle \rangle$ is the ensemble average.

The increase of MSD (mean square displacement) with time is related to the diffusion coefficient D .³⁷

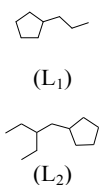
$$D = \frac{N_a}{6} \lim_{t \rightarrow \infty} \frac{d}{dt} \sum_{i=1}^{N_a} \langle [r_i(t) - r_i(0)]^2 \rangle \quad (2)$$

$$D = \frac{N_a}{6} \lim_{t \rightarrow \infty} \frac{d}{dt} \sum_{i=1}^{N_a} MSD \quad (3)$$

Where N_a is the number of diffusive atoms in the system, in Forcite module, The MSD is already averaged over all atoms and the relationship between the MSD and time has been fitted as a straight line, $y = a \cdot x + b$, D then follows as:

$$D = \frac{a}{6}$$

As we all know, it is difficult to carry out DFT calculation for the systems which are consisted with 1, 3 - didecyl cyclopentane, 1, 3 - dioctyldodecyl cyclopentane and atomic oxygen due to the extremely expensive computational price. However, the singlet and triplet atomic oxygen erosion mechanisms for alkylated cyclopentane can be investigated by DFT method. Therefore, we will choose the alkylated cyclic hydrocarbon models L_1 and L_2 shown as follow as our research objects.



The singlet and triplet atomic oxygen erosion mechanisms research on them will assist us to understand the atomic oxygen erosion mechanism of 1, 3 - didecyl cyclopentane and 1, 3 - dioctyldodecyl cyclopentane from the DFT perspective.

All calculations were completed through operating Gaussian 03 software,³⁸ and the hybrid density functional method B3LYP,³⁹ was adopted in our calculation and its accuracy has also been certified by many researches.⁴⁰⁻⁴³ Since five-membered ring exists in the research system and all species are neutral, polarized basis sets rather than diffuse basis should be chosen. Here, 6-311G (2d, 2p)⁴⁴ was used to carry out the geometric structure optimization. Reactants, intermediates and products were checked as the local minima after optimization calculation, and all transition states has been analysed in frequency (feature imaginary frequency) and certified by the intrinsic reaction coordinate (IRC) calculation again.^{45, 46}

Results and discussion

As Fig (2) shows, when large amounts of atomic oxygen contact with the 1, 3 - didecyl cyclopentane, 1, 3 - didecyl cyclopentane molecule is surrounded by atomic oxygen firstly.

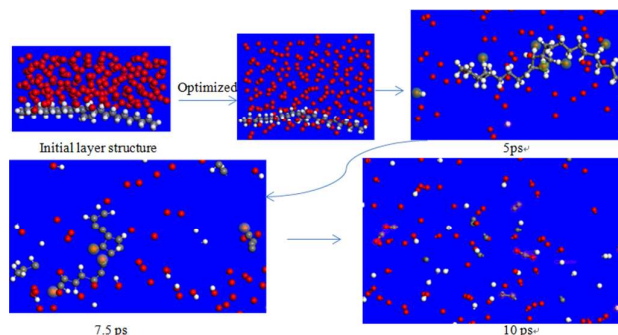


Fig 2. Reaxff MD simulation of atomic oxygen erosion process of 1, 3-didecyl cyclopentane.

Atomic oxygen interact with the H atoms of lubricant molecule and abstracts them away from the lubricant to form large amounts of $\text{OH}\cdot$, which can be clearly seen in the picture of 5ps (marked with the haloes). At 7.5 ps, the lubricant molecule was torn to some organic fragments. Meanwhile, atomic oxygen interacted with the C atoms of lubricant (marked with haloes). At 10 ps, the lubricant was completely damaged to create the H, $\text{OH}\cdot$, O_2 , CO, CO_2 and some small carbon clusters (marked with the cages).

As Fig 3 shows, when large amounts of atomic oxygen contact with 1, 3 - dioctyldodecyl cyclopentane, H atoms are also abstracted from lubricant molecule to form $\text{OH}\cdot$.

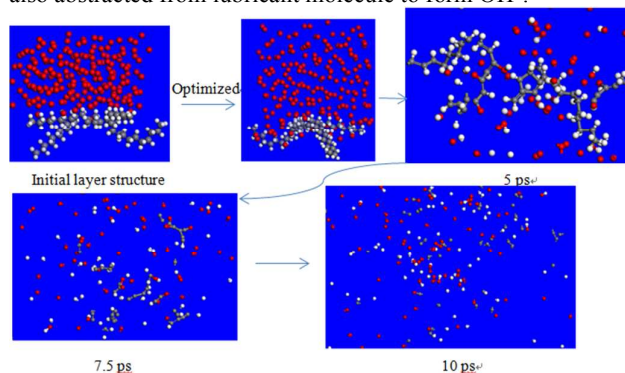
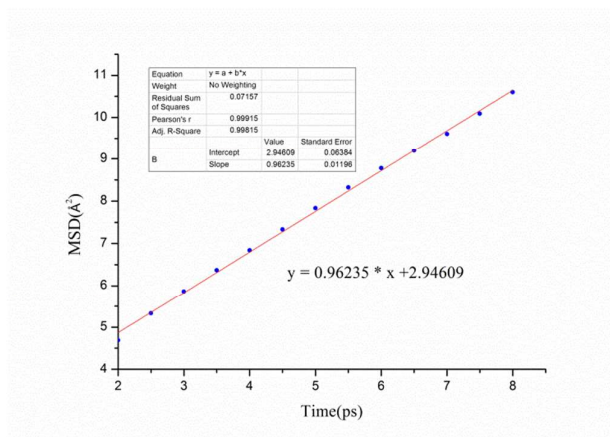


Fig 3. Reaxff MD simulation of atomic oxygen erosion process of 1, 3 - dioctyldodecyl cyclopentane

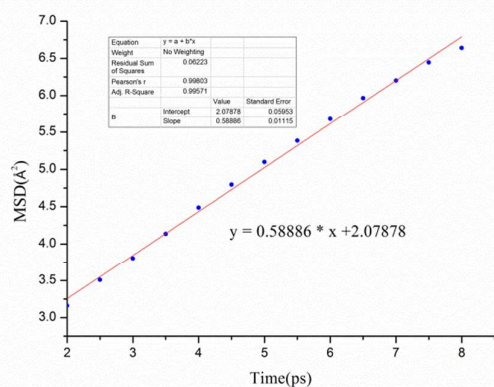
Different from the 1, 3 - didecyl cyclopentane, 1, 3 - dioctyldodecyl cyclopentane was broken down to several fragments by atomic oxygen at 5ps. These fragments are continually eroded by atomic oxygen until 7.5 ps, some carbon cluster appears and atomic oxygen continually interacts with them. Finally, 1, 3 - dioctyldodecyl cyclopentane was completely damaged to create H, H_2 , O_2 , CO, $\text{OH}\cdot$ and some small carbon clusters at 10 ps.

Here, noted that the creating of H and $\text{OH}\cdot$ and chain breakage are consistent with the preceding theoretical results of hydrocarbon eroded by triplet atomic oxygen.²⁰⁻²³

Until now, we cannot know the reason why 1, 3 - dioctyldodecyl cyclopentane has the better performance in preventing atomic oxygen erosion. However, the diffusion coefficient of atomic oxygen in two kinds of lubricants might give us a reasonable explanation. The relationship between MSD with time is show as Fig 4 (a, b).



(a)



(b)

Fig 4. (a) The relationship between MSD with time corresponds to atomic oxygen in 1, 3 - didecyl cyclopentane lubricant. (b) The relationship between MSD with time corresponds to atomic oxygen in 1, 3 - dioctyldecyl cyclopentane lubricant.

The diffusion coefficient of atomic oxygen in 1, 3 - didecyl cyclopentane is $0.16 \text{ \AA}^2/\text{ps}$, and it equals to $1.6 \times 10^{-5} \text{ cm}^2/\text{s}$. Meanwhile, the diffusion coefficient of atomic oxygen in 1, 3 - dioctyldecyl cyclopentane is $0.098 \text{ \AA}^2/\text{ps}$, and it equals to $9.8 \times 10^{-6} \text{ cm}^2/\text{s}$. The diffusion coefficient of atomic oxygen in 1, 3 - didecyl cyclopentane is 1.63 time than in 1, 3 - dioctyldecyl cyclopentane. Therefore, 1, 3 - dioctyldecyl cyclopentane lubricant with the better atomic oxygen resistance performance can be ascribed to the lower diffusion coefficient of atomic oxygen.

For hydrocarbon, in addition to the H-atom abstraction channel to produce $\text{OH}\cdot$, theory predicted that the H-atom abstraction and O-atom addition channels have comparable probabilities.²¹⁻²³ Furthermore, chain breaking appears to be entropically advantageous over hydrogen abstraction mechanisms.²⁰ Let us pay attention to the O-atom addition channels of L_1 and L_2 from the perspective of DFT calculation.

Gibbs free energy, relative Gibbs free energy of all intermediates and transition states, imaginary frequency of all transition states are shown in Table 1 of Electronic Supplementary Information. All reaction potential surfaces are included in Figs 3-16 of Electronic Supplementary Information.

^3O erosion mechanism for L_1

As Fig 5 shows, triplet atomic oxygen firstly attacks the L_1 , the initial compound is $^3\text{IM}1$, and then going through transition state $^3\text{TS} 1$ to form $^3\text{IM}2$, the activation barrier of this process was 2.32 eV, and the products are $\text{C}_5\text{H}_9\cdot$ and $\text{C}_3\text{H}_7\text{O}\cdot$.

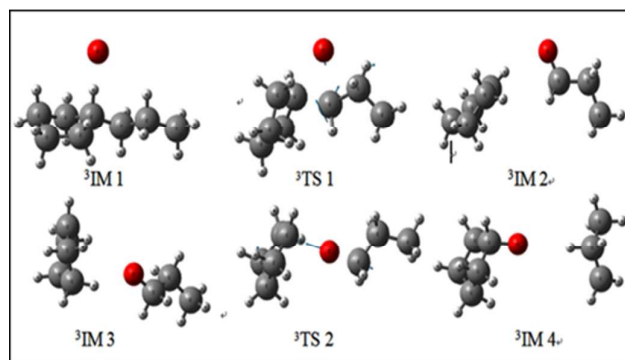


Fig 5. The optimized geometries of all intermediates and transition states correspond to $L_1 + ^3\text{O} \rightarrow \text{C}_5\text{H}_9\text{O}\cdot + \text{C}_3\text{H}_7\cdot$.

Meanwhile, there is also an oxygen exchange process between $\text{C}_5\text{H}_9\cdot$ and $\text{C}_3\text{H}_7\text{O}\cdot$. $^3\text{IM}3$ was formed after the spatial configuration re-modifying of $\text{C}_5\text{H}_9\cdot$ and $\text{C}_3\text{H}_7\text{O}\cdot$, after that, $^3\text{IM}3$ goes through $^3\text{TS} 2$ which has an oxygen transfer characteristics to generate $^3\text{IM}4$ with an activation barrier of 3.79 eV and it is an endothermic process. Finally, $\text{C}_5\text{H}_9\text{O}\cdot$ and $\text{C}_3\text{H}_7\cdot$ are generated.

$\text{C}_3\text{H}_7\cdot$, $\text{C}_3\text{H}_7\text{O}\cdot$, $\text{C}_5\text{H}_9\cdot$, and $\text{C}_5\text{H}_9\text{O}\cdot$ have created through the above two courses.

As Fig 6 shows, $\text{C}_3\text{H}_7\text{O}\cdot$ goes through the $^2\text{TS} 3$ to form $^2\text{IM} 5$, the final products are $\text{C}_2\text{H}_5\cdot$ and CH_2O . This is a C-C σ bond breakage course in the style of stretching, and the activation barrier is 0.95 eV, which is also an endothermic course.

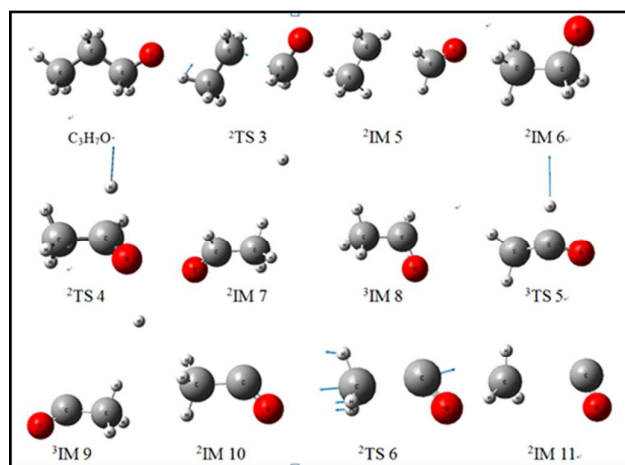


Fig 6. The optimized geometries of all intermediates and transition states correspond to $\text{C}_3\text{H}_7\text{O}\cdot + ^3\text{O} \rightarrow \text{CH}_2\text{O} + \text{H} + \text{CO} + \text{CH}_3\cdot$.

The formed $\text{C}_2\text{H}_5\cdot$ is attacked by another ^3O to form $^3\text{IM}6$ ($\text{C}_2\text{H}_5\text{O}\cdot$). Hence, two dehydrogenation processes occur, in which the corresponding transition states are $^2\text{TS} 4$ and $^3\text{TS} 5$, and the corresponded activation barrier of these two processes are 1.05 and 0.94 eV. $^2\text{IM} 10$ ($\text{C}_2\text{H}_3\text{O}\cdot$) and H are generated.

$^2\text{IM}10$ ($\text{C}_2\text{H}_3\text{O}\cdot$) goes through $^2\text{TS} 6$ to form the final products CO and $\text{CH}_3\cdot$. It is necessary to surmount an activation barrier of 0.67 eV and extra energy supply of 0.44 eV.

Until now, we found that the side chain was eroded by ^3O to create H and CO and CH_2O .

The ^3O erosion course of $\text{C}_5\text{H}_9\text{O}\cdot$ should be noted here. As Fig 7 shows,

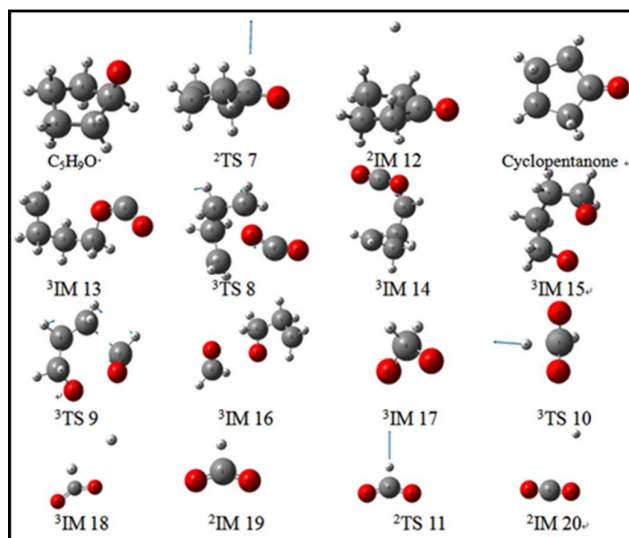


Fig 7. The optimized geometries of all intermediates and transition states correspond to $C_5H_9O\cdot + {}^3O \rightarrow H + CO_2$.

$C_5H_9O\cdot$ surmounts 3TS7 and takes off H to form cyclopentanone by overcoming an activation barrier of 0.95 eV, with an endothermic energy 0.47 eV. One more 3O continuously attacks cyclopentanone, 3O inserts among the C-C bond of cyclopentanone, leading to the breakage of another C-C bond and the forming of ${}^3IM 13$, which can be taken as the tearing course of five-membered ring. ${}^3IM 13$ goes through the ${}^3TS 8$ with an oxygen abstraction characteristic to create CO_2 and $\cdot C_4H_8\cdot$ di-radical, by overcoming an activation barrier of 4.17 eV. Thus, it is demonstrated that H and CO_2 can be created from the 3O erosion of $C_5H_9O\cdot$.

After the tearing of the five-membered ring, the formed $\cdot C_4H_8\cdot$ di-radical combines with two more 3O to form $\cdot OC_4H_8O\cdot$ (3IM15). The following course is still the stretching and breaking of the C-C bond to form formaldehyde, and this trend could be seen from the ${}^3TS 9$, the activations barrier of the C-C bond cleavage is 0.63 eV with endothermic energy 0.16 eV. Namely, the CH_2 units are easily to be taken off. Therefore, the side chain can be eroded in the unit of CH_2O as more 3O attacks. In other word, 3O erosion of hydrocarbon di-radical will generate large amounts of CH_2O .

As known from the above, large amounts of CH_2O were generated during the 3O erosion course. The products of 3O oxidation of CH_2O are CO_2 and H rather than $HCOOH$ as shown in Fig 7. Two dehydrogenation courses correspond to the ${}^3TS 10$ and ${}^3TS 11$, the activation barrier of these two course are 0.45 and 0.24 eV respectively, and the reaction heats were 0.10 eV and 0.26 eV respectively. Here, another origination of CO_2 was found, which comes from the 3O oxidation of CH_2O .

3O erosion mechanism for L_2

For the triplet atomic oxygen erosion of L_2 , initial compound was 3IM21 , followed by the inserting of 3O and creating of $C_3H_7\cdot$ and $C_9H_{17}O\cdot$. The tendency of oxygen inserting can be demonstrated clearly by 3TS12 shown in Fig 8.

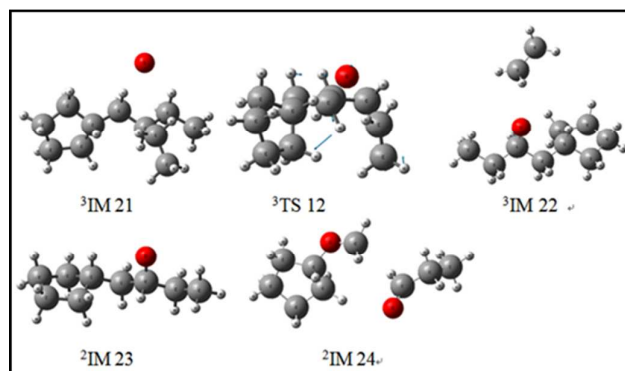


Fig 8. The optimized geometries of all intermediates and transition states correspond to the 3O erosion process of L_2 .

This process has an activation barrier of 2.28 eV and the reaction heat was 0.92 eV. Here, noted that the activation barrier of this C-C bond is lower than the C-C bond in L_1 by 25.10 kcal / mol. In other words, the C-C bond connects main side chain and branched chain was easier to be broken. Thus, the branched chain is firstly taken off.

When $C_9H_{17}O\cdot$ undergoes another 3O attacking, it is found that the C-C bond in main side chain of $C_9H_{17}O\cdot$ is broken, only stable species such as 2IM24 exists. From the above information, we can infer that 3O attacks $C_9H_{17}O\cdot$ mainly in the way of O-atom inserting to break the C-C bond, producing some hydrocarbon aldehyde and organic oxygen free radicals. From here we can clearly see the atomic inserting mechanism.

1O erosion mechanism for L_1

As shown in Fig 9, 1O collides with L_1 and inserts among the C-H bond to form the stable intermediate 1IM1 , followed by transition state ${}^1TS 1$ with a characteristic of hydrogen transfer to reach 1IM2 . This process has activation energy of 2.57 eV and is endothermic with 0.25 eV, the final products are H_2O and unsaturated hydrocarbon. The formed unsaturated hydrocarbon undergoes two more 1O attacking, producing two stable organic epoxy compounds 1IM3 and 1IM4 . No free radicals are generated in the whole process, and the C-H bonds are activated instead of C-C bonds. Therefore, it can be inferred that the lubrication performance can be well maintained if large amounts of atomic oxygen in low earth orbital are singlet because the erosion extent of singlet atomic oxygen is slighter and the products are approximate to the lubricant itself.

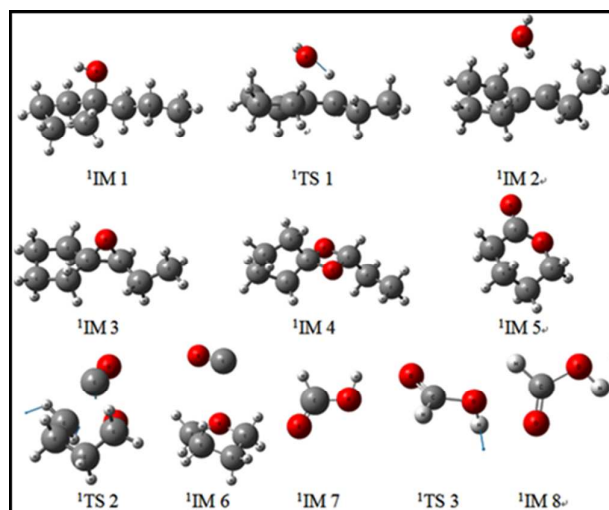


Fig 9. The optimized geometries of all the intermediates and transition states correspond to ^1O erosion of L_1 , formaldehyde and cyclopentanone.

^1O oxidation of cyclopentanone and CH_2O

In view of cyclopentanone and CH_2O are two products of ^3O erosion of L_1 , the ^1O oxidation process of these two species rose our interesting. As Fig 9 shows, different from the ^3O erosion, the cyclopentanone was not damaged during the inserting course of ^1O . The initial complex $^1\text{IM} 5$ goes through the $^1\text{TS} 2$ to form $^1\text{IM}6$, and CO and $\text{C}_4\text{H}_8\text{O}$ were created. It is necessary to surmount an activation barrier of 4.17 eV. Something needs to be emphasized that the product was CO rather than CO_2 .

Similarly, ^1O oxidation processes of CH_2O have been investigated. The *cis*- HCOOH as initial product is formed in the manner of atomic inserting once ^1O attacking (Fig 9). However, *cis*- HCOOH goes through the $^1\text{TS} 3$ which has a feature of swing to form the more stable *trans*- HCOOH . No CO and H are generated in the whole oxidation process, and the activation barrier is 0.35 eV and the reaction heat is 0.21 eV. From the perspective of kinetics and thermodynamics, this structural transformation is extremely easy to occur. Here, a conclusion can be drawn that ^3O and ^1O respectively corresponds to the extremely different erosion mechanism.

Fig 10 demonstrates the schematic diagram of electron spin-flip mechanism due to the spin-orbit coupling. The prerequisite of spin-flip is that there must have been different spin states which have almost identical energy mixed together. However, there are not the same reaction mechanisms, and it will not appear the extremely similar molecular structure corresponding to the identical energy. Thus, this is one of the reasons why there is no non-adiabatic reaction process.

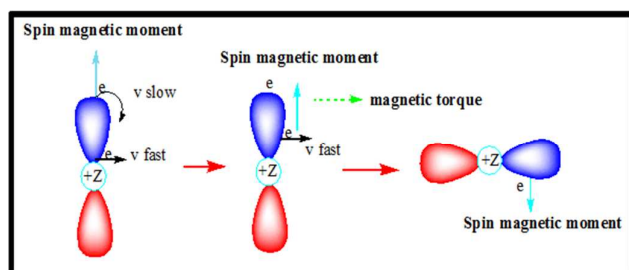


Fig 10. The scheme corresponds to spin-flip advanced by spin-orbit coupling.

Furthermore, the atomic oxygen is either in the style of free radical forming or saturated covalent bond. Therefore, the freedom degree of electrons is restricted. In other words, atomic oxygen cannot provide the orbitals and electrons for spin-flip caused by the spin-orbit coupling.

Theoretical analysis of bonds activation

As for the C-C bond activation in L_1 . Firstly, the different electrons configuration of ^1O and ^3O leads to the different erosion mechanisms. ^3O has unpaired electron and can bond to C atom and ^1O can only support empty orbital. Thus, HOMO of L_1 embraces the bond orbital of C-C bond, LUMO of ^3O contacts with HOMO of L_1 , the electrons in HOMO of R_1 transfers to LUMO of ^3O , making the electron density of bonding orbital decrease and resulting in the activation of C-C bond (Fig 11(d)). Meanwhile, we can clearly see the H atom can be abstracted by triplet atomic oxygen from the Fig 11(d), which is consistent with the Reaxff MD simulation results.

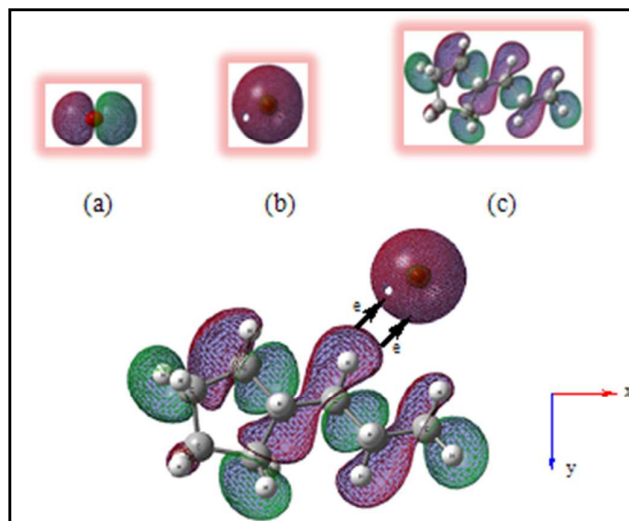


Fig 11. (a) LUMO of ^1O . (b) LUMO of ^3O . (c) HOMO of R_1 . (d) The erosion mechanism of C-C bond by ^3O .

As for the activation of C-H bond, LUMO of ^1O was p orbital and symmetry matches with the sp^3 orbital of C-H bond. Therefore, atomic oxygen can insert in the C-H bond. It was likely to be connected to another C-H bond orbital after oxygen insert, electrons in C-H orbital would transfer to the LUMO of ^1O , and thus leading to the activation of C-H bond and dehydration.

As for the breaking off of the branched chain in L_2 , the initial complex $^3\text{IM}21$, Muliken charge on C and O were -0.038 and -0.042 respectively. However, in $^3\text{TS}12$, Muliken charge on C and O were -0.002 and -0.294 respectively. It is clearly demonstrated that negative charges on C has reduced and the negative charges on O have increased. It is probably due to the electron donating characteristic of branched chain alkyl makes the electron density increase in C-C bond which connects the main chain and branched chain. The oxygen atoms are more likely to attack the electronegative position, the electron in C-C bond will transfer to the LUMO of ^3O and C-C bond will be activated.

Conclusions

In this work, the micro erosion processes of large amounts of atomic oxygen for 1, 3 - didecyl cyclopentane and 1, 3 - dioctyldecyl cyclopentane lubricants have been investigated utilizing Reaxff molecular dynamics. Singlet and triplet atomic oxygen erosion mechanisms for L_1 and L_2 have been studied by density functional theory (DFT) method.

For two kinds of space lubricants, the main erosion ways are H abstraction and chain breakage due to O-atom addition. The creating of CO , CO_2 , and H_2 is the main reason for the quality loss of lubricants.

1, 3 - dioctyldecyl cyclopentane lubricant has the better atomic oxygen resistance performance because of the lower atomic oxygen diffusion coefficient. The more branched chains in lubricant molecule the better performance in preventing atomic oxygen, because it can hinder the atomic oxygen diffusion in lubricant.

For the alkylated cyclopentane L_1 , the whole main side chain is firstly taken off due to the addition of triplet atomic oxygen. The five-membered ring can be completely tore and eroded. For the L_2 with the branched chain, the branched chain will be firstly taken off due to the lower activation barrier.

Alkylated cyclopentane is attacked by singlet atomic oxygen to create H_2O and unsaturated double bond organic compounds as initial products, and corresponds to elimination mechanism.

Organic epoxide will be formed if more ^1O attacking. In one word, ^1O erosion has a little damage on lubricant molecule.

Different spin states atomic oxygen corresponds to the different erosion mechanism. The reaction does not appear the non-adiabatic reaction process, which is attributed to atomic oxygen existing either in hydrocarbon radical or saturated bonds, restricting the freedom degrees of electrons.

Acknowledgements

This work is supported by the National Nature Science Foundation of China (NO 11172301 and 21203217), the “Funds for Distinguished Young Scientists” of Hubei Province (2012FFA002), the “Western Light Talent Culture” Project, the Co-joint Project of Chinese Academy of Sciences and the “Top Hundred Talents” Program of Chinese Academy of Sciences and the National 973 Project (2013CB632300) for financial support.

Notes and references

^a State Key laboratory of Solid Lubrication, Lanzhou Institute of Chemical Physics, Chinese Academy of Sciences, Lanzhou 730000, China.

^b Hubei Collaborative Innovation Centre for Advanced Organic Chemical Materials and Ministry of Education Key Laboratory for the Green Preparation and Application of Functional Materials, Hubei University, Wuhan 430062, People’s Republic of China.

^c College of Chemistry and Chemical Engineering, Northwest Normal University, Lanzhou 730070, China

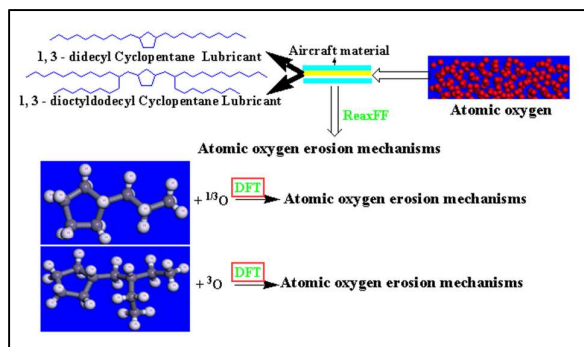
*The corresponding author, Fax: 0086-931-8277088; Tel: 0086-931-4968105; E-mail: zgou@licp.cas.cn

Electronic Supplementary Information (ESI) available: Structure of linear conjugated perfluoropolyether fragment (PFPE); Three Confined Shear simulation model, linear conjugated perfluoropolyether, 1, 3-didecyl cyclopentane and 1, 3-dioctyl dodecyl cyclopentane as lubricants; Frictional coefficient curve corresponds three different lubricants; Gibbs free energy, relative Gibbs free energy of all the intermediates and transition states, imaginary frequency of all transition states; All reaction potential surfaces. See DOI: 10.1039/b000000x/

- 1 U.S. Standard Atmosphere, 1976, NOAA-S/T 76-1562; National Oceanic and Atmospheric Administration, National Aeronautics and Space Administration, and the United States Air Force, U.S. Government Printing Office: Washington, DC, 1976.
- 2 B. A. Banks, K. K. de Groh, S. Rutledge, F. J. DiFilippo, Prediction of In-Space Durability of Protected Polymers Based on Ground Laboratory Thermal Energy Atomic Oxygen; NASA TM-107209; National Aeronautics and Space Administration: Washington, DC, 1996
- 3 D. Dooling, M. M. Finckenor, Material Selection Guidelines to Limit Atomic Oxygen Effects on Spacecraft Surfaces; NASA/TP-1999-209260; National Aeronautics and Space Administration: Washington, D.C., 1999.
- 4 T. K. Minton, D. J. Garton, Dynamics of Atomic-Oxygen-Induced Polymer Degradation in Low-Earth Orbit. In Advanced Series in Physical Chemistry 11: Chemical Dynamics in Extreme Environments; Dressler, R. A., Ed.; World Scientific: Singapore, 2001, 420.
- 5 B. A. Banks, K. K. de Groh, S. K. Miller, Low Earth Orbital Atomic Oxygen Interactions with Spacecraft Materials; NASA/TM-2004-213400; National Aeronautics and Space Administration: Washington, D.C., 2004.
- 6 J. Dever, B. Banks, K. de Groh, S. Miller, Degradation of Spacecraft Materials. In Handbook of Environmental Degradation of Materials; Kutz, M., Ed.; William Andrew Publishers: Norwich, NY, 2005, 23, 465.
- 7 K. K. de Groh, B. A. Banks. Techniques for Measuring Low Earth Orbital Atomic Oxygen Erosion of Polymers. In 2002 Symposium and Exhibition Sponsored by the Society for the Advancement of Materials and Process Engineering; Long Beach, CA, May 12–16, 2002; Society for the Advancement of Materials and Process Engineering: Covina, CA, 2002.

- 8 B. A. Banks, C. A. Karniotis, D. Dworak, M. Soucek, Atomic oxygen durability evaluation of a UV curable ceramer protective coating. *NASA*, 2004.
- 9 T. Li, L. X. Jiang, W. Q. Feng, X. P. Liu, *Spacecraft Environment Engineering*, 2009, **26**, 222.
- 10 A. Gindulyte, L. Massa, B. A. Banks, S. K. Rutledge, *J. Phys. Chem. A*, 2000, **104**, 9976.
- 11 A. Gindulyte, L. Massa, *J. Phys. Chem. A*, 2002, **106**, 5463.
- 12 D. Troya, R. Z. Pascual, G. C. Schatz, *J. Phys. Chem. A*, 2003, **107**, 10497.
- 13 J. M. Zhang, H. P. Upadhyaya, A. L. Brunsvold, T. K. Minton, *J. Phys. Chem. B*, 2006, **110**, 12500.
- 14 D. J. Garton, T. K. Minton, *J. Phys. Chem. A*, 2009, **113**, 4722.
- 15 M. Ray, B. Saha, G. C. Schatz, *J. Phys. Chem. C*, 2012, **116**, 26577.
- 16 X. L. Wang, X. J. Sun, T. T. Gao, *Tribology*, 2010, **30**, 425.
- 17 J. Braza, M. J. Jansen, W. R. Jones, *NASA/CR*, 2009, **21**, 5637.
- 18 P. Gao, L. Peng, D. P. Feng, W. M. Liu, *Tribology*, 2011, **32**, 428.
- 19 P. Gao, L. Peng, W. M. Liu, *Tribology*, 2011, **31**, 1.
- 20 D. J. Garton, T. K. Minton, D. Troya, R. Pascual, G. C. Schatz, *J. Phys. Chem. A*, 2003, **107**, 4583.
- 21 D. Troya, R. Z. Pascual, G. C. Schatz, *J. Phys. Chem. A*, 2003, **107**, 10497.
- 22 A. Gindulyte, L. Massa, B. A. Banks, S. K. Rutledge, *J. Phys. Chem. A*, 2000, **104**, 9976.
- 23 D. Troya, R. Z. Pascual, D. J. Garton, T. K. Minton, G. C. Schatz, *J. Phys. Chem. A*, 2003, **107**, 7161.
- 24 S. Shaik, D. Danovich, A. Fiedler, D. Schröder, H. Schwarz, *Helv. Chem. Acta*, 1995, **78**, 1393.
- 25 D. Danovich, S. Shaik, *J. Am. Chem. Soc.*, 1997, **119**, 1773.
- 26 J. Y. Nian, Y. C. Wang, W. P. Ma, D. F. Ji, C. L. Wang, M. J. La, *J. Phys. Chem. A*, 2011, **115**, 11023.
- 27 Y. C. Wang, Q. Wang, Z. Y. Geng, L. L. Lv, Y. B. Si, Wang, Q. Y., H. W. Liu, D. D. Cui, *J. Phys. Chem. A*, 2009, **113**, 13808.
- 28 L. L. Lv, Y. C. Wang, Q. Wang, H. W. Liu, *J. Phys. Chem. C*, 2010, **114**, 17610.
- 29 J. Y. Nian, L. Tie, B. Wang, Z. G. Guo, *J. Phys. Chem. A*, **2013**, **117**, 8843–8854.
- 30 A. C. T. van Duin, S. Dasgupta, F. Lorant, W. A. Goddard, *J. Phys. Chem. A*, 2001, **105**, 9396.
- 31 R. M. Abolfath, K. Cho, *J. Phys. Chem. A*, 2012, **116**, 1820.
- 32 M. Zheng, X. X. Li, J. Liu, L. Guo, *Energy Fuels*, 2013, **27**, 2942.
- 33 S. Y. Kim, N. Kumar, P. Persson, J. Sofo, A. C. T. van Duin, J. D. Kubicki, *Langmuir*, 2013, **29**, 7838.
- 34 T. T. Qi, C. W. B. Jr, J. W. Lawson, T. G. Desai, E. J. Reed, *J. Phys. Chem. A*, 2013, **117**, 11115.
- 35 M. Raju, S. Y. Kim, A. C. T. van Duin, K. A. Fichthorn, *J. Phys. Chem. C*, 2013, **117**, 10558.
- 36 H. Sun, *J. Phys. Chem. B*, 1998, **102**, 7338.
- 37 M. Meunier, *J. Chem. Phys.*, 2005, **123**, 134906.
- 38 M. J. Frisch, et al. *GAUSSIAN 03, revision E.01*; Gaussian Inc: Pittsburgh, PA, 2003.
- 39 A. D. Becke, *J. Chem. Phys.*, 1993, **98**, 1372.
- 40 H. G. Cho, L. Andrews, *J. Am. Chem. Soc.*, 2005, **127**, 8226.
- 41 Z. Guo, Z. F. Ke, D. L. Phillips, C. Y. Zhao, *Organometallics*, 2008, **27**, 181.
- 42 K. J. deAlmeida, A. Cesar, *Organometallics*, 2006, **25**, 3407.
- 43 E. D. Santo, M. C. Michelini, N. Russo, *Organometallics*, 2009, **28**, 3716.
- 44 A. D. McLean, G. S. Chandler, *J. Chem. Phys.*, 1980, **72**, 5639.
- 45 C. Gonzalez, H. B. Schlegel, *J. Chem. Phys.*, 1989, **90**, 2154.
- 46 C. Gonzalez, H. B. Schlegel, *J. Chem. Phys.*, 1990, **94**, 5523.

Table of Contents



Atomic Oxygen Erosion Mechanisms of 1, 3 -
Didecyl Cyclopentane, 1, 3 - Dioctyldecyl
Cyclopentane and Alkylated Cyclopentane